Advances in Engineering Software 100 (2016) 97–112

Contents lists available at ScienceDirect

Advances in Engineering Software

journal homepage: www.elsevier.com/locate/advengsoft

Topology optimization with manufacturing constraints: A unified projection-based approach

Sandro L. Vatanabe[a], Tiago N. Lippi[a], Cícero R. de Lima[b,*], Glaucio H. Paulino[c], Emílio C.N. Silva[a]

[a] Department of Mechatronics and Mechanical Systems Engineering, USP – University of São Paulo, Av. Prof. Mello Moraes, 2231, São Paulo, SP, 05508-900, Brazil
[b] School of Engineering, Modeling and Applied Sciences/UFABC – Federal University of ABC, Rua Arcturus, 03, São Bernardo do Campo, SP, 09606-070, Brazil
[c] School of Civil and Environmental Engineering, GeorgiaTech – Georgia Institute of Technology, 790 Atlantic Drive NW, Atlanta, GA 30332-0355, USA

ARTICLE INFO

Article history:
Received 22 March 2016
Revised 7 June 2016
Accepted 11 July 2016
Available online 25 July 2016

Keywords:
Topology optimization
Projection scheme
Manufacturing constraints
Minimum member size
Minimum hole size

ABSTRACT

Despite being an effective and a general method to obtain optimal solutions, topology optimization generates solutions with complex geometries, which are neither cost-effective nor practical from a manufacturing (industrial) perspective. Manufacturing constraint techniques based on a unified projection-based approach are presented herein to properly restrict the range of solutions to the optimization problem. The traditional stiffness maximization problem is considered in conjunction with a novel projection scheme for implementing constraints. Essentially, the present technique considers a domain of design variables projected in a pseudo-density domain to find the solution. The relation between both domains is defined by the projection function and variable mappings according to each constraint of interest. The following constraints have been implemented: minimum member size, minimum hole size, symmetry, pattern repetition, extrusion, turning, casting, forging and rolling. These constraints illustrate the ability of the projection scheme to efficiently control the optimization solution (i.e. without adding a large computational cost). Illustrative examples are provided in order to explore the manufacturing constraints in conjunction with the unified projection-based approach.

1. Introduction

This paper addresses manufacturing constraints by means of a *unified projection-based approach* restricting the range of solutions to the topology optimization problem. A domain of design variables is considered, which is projected in a pseudo-density domain to obtain the solution. The relation between domains is defined by the projection and variable mappings according to each manufacturing constraint of interest. The following constraints are considered: minimum member size, minimum hole size, symmetry, extrusion, pattern repetition, turning, casting, forging, and rolling.

Fig. 1 illustrates the relationship between the manufacturing techniques and the manufacturing constraints implemented. The figure shows the necessary manufacturing constraints in order to generate compatible designs for each manufacturing technique. It also relates each manufacturing technique to the pertinent manufacturing constraints that can be applied. For example, minimum member size, minimum hole size, symmetry, and pattern repetition constraints are apllied to allow a part be manufactured by the milling process. In summary, Fig. 1 illustrates the guiding philosophy of the present work.

This article is organized as follows. Section 2 presents the background and the state of the art in the field in order to place the present work in a proper context. Section 3 presents a brief overview of the topology optimization concepts. Section 4 describes the main idea associated with the projection and mapping techniques employed. Section 5 presents the actual manufacturing constraints addressed in this work. Section 6 provides details concerning the numerical implementation of manufacturing constraints and regarding the topology optimization procedure. Section 7 presents projection-based results associated with a diversity of examples. Finally, in Section 8, conclusions are inferred and the potential extensions of this work are indicated.

2. Background and state of the art

Topology optimization is a powerful tool to design effective and efficient structures. In the past few years, significant improvements have been made in order to improve the technique, such as development of filters based on gradients [1], image processing [2], and

* Corresponding author. Fax: +551149960089.
E-mail address: cicero.lima@ufabc.edu.br (C.R.d. Lima).

http://dx.doi.org/10.1016/j.advengsoft.2016.07.002
0965-9978/

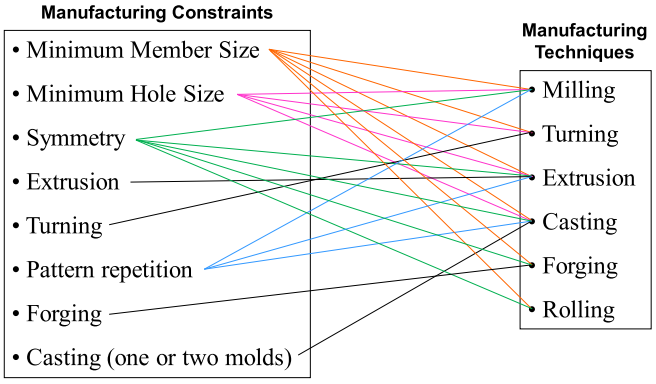

Fig. 1. Manufacturing constraints relationship scheme illustrating the philosophy of the present work.

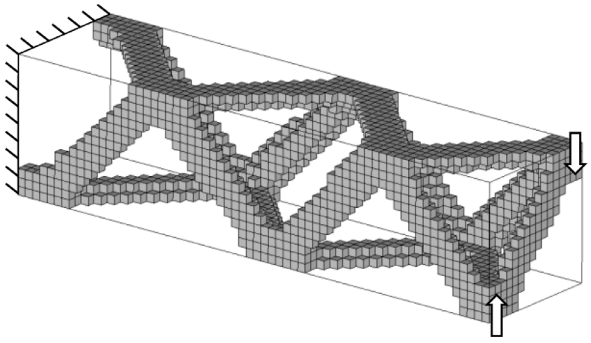

Fig. 2. Example of a complex solution obtained by using the topology optimization method – cantilever domain subjected to a torsion load at the end.

other procedures aiming at solving the long-standing checkerboard problem, the non-uniqueness of solutions, and the gray scale [3]. Even when the aforementioned techniques are employed, a major problem remains, which is the complexity of the obtained solutions, as illustrated in Fig. 2.

Synthesis of structures by means of topology optimization may lead to complex shapes (Fig. 2) and, in general, are neither cost-effective nor practical to manufacture. A common procedure consists of post-processing the result by interpolation functions and smoothening of curves/shapes [1]. Sometimes, in order to achieve a practical solution, the original design needs to be substantially modified, losing its optimized characteristics. This problem has motivated the topology optimization community to seek solutions tailored for specific manufacturing processes [4–11]. These solutions are useful for both traditional and additive manufacturing processes; however, the focus of this paper lies on the latter. References addressing the connection between additive manufacturing and topology optimization can be found in Leary et al. [12].

The approach of this work consists in defining the constraints of an optimization problem, by employing projection techniques [13,14] tailored to meet the requirements of the manufacturing processes, thus, simplifying the process of interpreting topology optimization solutions. The current tendency to develop a product cycle leads to procedures in which design, simulation, and optimization with manufacturing constraints can be simultaneously executed in computer-aided engineering (CAE) phase design [15], instead of the traditional procedures, in which the design and optimization are developed separately, in computer-aided design (CAD) and CAE phases, respectively. Final shapes with high resolution incorporating manufacturing constraints can be obtained by adopting highly discretized FEM models [16], reducing time and product development cost.

Previous works have addressed manufacturing constraint techniques. For instance, Zuo et al. [4] considered manufacturing and machining factors in the topology optimization problem. They introduced manufacturing constraints according to requirements for different applications. Harzheim and Graf [5] compared the topology optimization of cast parts with and without manufacturing constraints, and observed better results for cast part design when a minimum thickness control is included in the optimization problem. Ishii and Aomura [6] proposed a methodology based on the homogenization method to produce optimized structures with constant cross section, which is easily manufactured by extruding. An alternative method to design continuum structures subjected to extrusion constraints was developed by Lia et al. [7], who combined a parametric level set method with a discrete wavelet transform approximation for this purpose. Gersborg and Andreasen [8] applied the Heaviside design parametrization to obtain manufacturable cast designs in a gradient driven topology optimization. Later, Zhu et al. [9] proposed an alternative linear interpolation to allow the topology optimization of large-scale stretch-forming die designs. Sørensen and Lund [10] included explicit manufacturing constraints to topology and thickness optimization of laminated composites as a large number of sparse linear constraints. Wang et al. [11] demonstrated that the local length scale control in topology optimization is difficult to obtain by employing simple projection filtering techniques. Therefore, they proposed a modified robust topology optimization formulation that combines three projection schemes into a min-max problem to overcome this difficulty, however, at a high computational cost.

In contrast, a novel integrated approach is proposed herein, combining a projection technique with a mapping technique, in which different kinds of manufacturing constraints are implemented in the topology optimization process. The goal is to achieve feasible engineering solutions, with smaller computational effort, which can be fabricated by means of well-known and well-controlled manufacturing processes [17].

3. A few remarks on topology optimization

In a general sense, topology optimization leads to optimized structures by means of optimization algorithms that provide a distribution of mass within a design domain. Some of the optimization algorithms commonly employed include Sequential Linear (or Quadratic) Programming [18], Method of Moving Asymptotes [19], and Optimality Criteria [1], to name a few.

The topology optimization method employs some basic concepts such as a fixed design domain and relaxation of the optimization problem [1]. The latter consists in solving the problem in a continuum form, rather than addressing the original 0-1 (void-solid) problem in discrete form. Usually, the domain is discretized with the Finite Element Method [20] and the problem is solved based on the sensitivities obtained for the optimization cycle by means of a proper material model. Various material models have been proposed in the literature [1]. Here, the so-called SIMP model (Solid Isotropic Material with Penalization) [21,22] is applied, using penalization coefficients on the pseudo-densities (ρ) of each element in order to reduce intermediate regions that appear due to relaxation, as follows:

$$\boldsymbol{C}^H = \rho^p \boldsymbol{C}_0 \tag{1}$$

where C^H is the resulting stiffness tensor, p is the penalization factor, and C_0 is the tensor for the basic isotropic material used. In this process, intermediate pseudo-densities and checkerboard instability appear in the solution. To address such problems, complexity control such as filters [2] and projection techniques [13] have been the solution of choice in the technical litera-

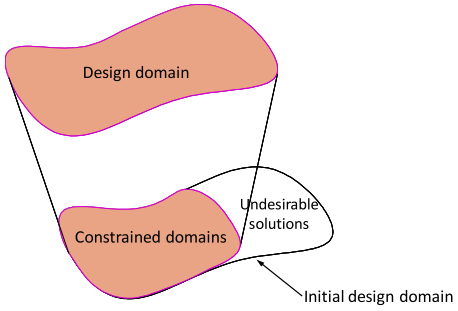

Fig. 3. Original and constrained domain through projection.

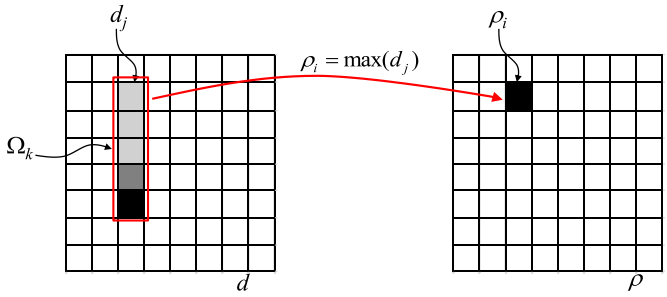

Fig. 5. Projection scheme of variables d_j onto the pseudo-densities domain ρ by using Eq. (2).

ture. Here, a different approach is applied, based on the projection scheme proposed by Le [14], as addressed in the next Section.

4. Projection technique

Projection schemes consist in projecting a design variables domain onto a pseudo-densities domain to exclude undesirable solutions of optimization problem, as illustrated in Fig. 3. This technique is utilized in [13] to achieve minimum length scale on structural members generated by topology optimization, and to circumvent mesh-dependency and checkerboard problems.

The projection scheme can also drive the topology optimization problem to solutions with desirable geometry characteristics, easily restricting the problem and avoiding more complicated formulations that induce very complex problems, which probably require high computational time. In this work, projection and mapping techniques are combined for generating manufacturing constraints that result in topologies with geometrical features that are amenable to traditional manufacturing processes, such as extrusion, milling, casting, turning, forging, and rolling.

The effect of the projection scheme is to reduce the solution domain by searching other desired space of variables. To apply this technique three steps are necessary: (1) mapping the relation between design variables (d) and pseudo-densities (ρ) domains; (2) projecting the design variables domain onto the pseudo-densities domain to achieve the solution; and (3) calculation of the pseudo-densities sensitivity in relation to the design variables sensitivity.

4.1. Domain variable mappings

The mapping relation of both domains (d and ρ) identifies which elements in the pseudo-densities domain (ρ) are influenced by the design variables domain (d) [14]. This mapping is carried out by obeying a procedure established by the problem formulation, which varies according to the required manufacturing constraint as discussed in the next Section. For instance, Fig. 4 shows a mapping procedure of all elements d_j (belonging to a predefined Ω_k region in domain d) in a pseudo-densities domain ρ, following an adopted direction coordinate (+X). This mapping procedure (Fig. 4) is adopted for numerical implementation of various manufacturing constraints (casting, turning, forging, and rolling) described ahead in the Section 6.

Since it is noticed that there is more than one variable d projected on the same pseudo-density ρ, a procedure for deciding what value will be adopted is required. In this case, the maximum value is adopted, as shown in next Section. This step of projection procedure has a relatively high computational cost. However, if the projection procedure does not change during the problem solution, the mapping step can be performed only once at beginning of the optimization problem, thus reducing the computational time.

In this sense, the mapping procedure adopted in this projection differs from the mapping used in the projection proposed by Guest et al. [13], in which essentially a set of design variables located inside a predefined circular region (Ω_k), in the design variable space (d), is mapped to just one design variable in the pseudo-density space (ρ), by using Heaviside functions [23]. Here, design variables located inside either circular or rectangular regions (Fig. 5) can be applied to this mapping, according to the kind of manufacturing constraint employed in the topology optimization problem.

4.2. Projecting domain variables

At this step, variables d_j are calculated and projected onto the domain of pseudo-densities (ρ_i) by using a projection function at

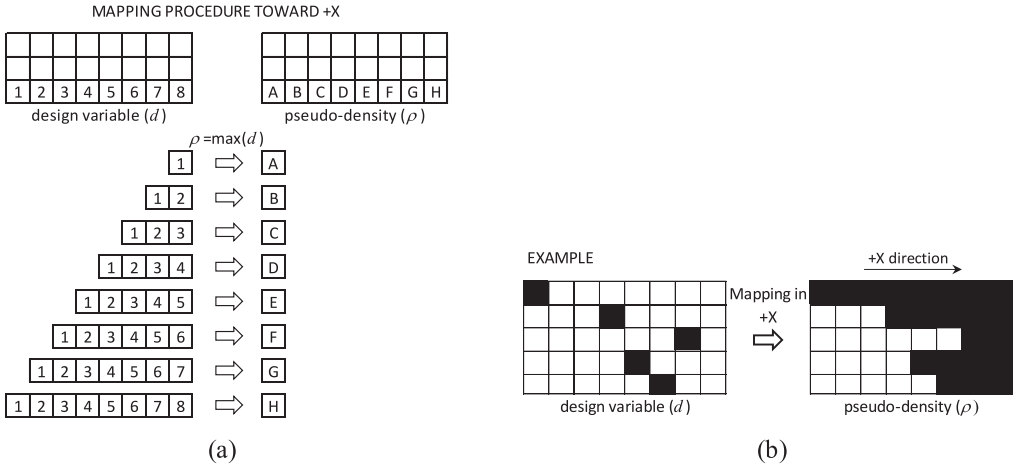

Fig. 4. Mapping relation between design variable (d) and pseudo-density (ρ) domains: (a) schematic mapping procedure; (b) example of mapping of both domains (d and ρ).

each iteration of the topology optimization process. As previously mentioned in the mapping procedure (Section 4.1), the maximum value of a set of variables d_j is required for projecting variables, i.e. $\rho_i = \max(d_j)$. Here, this max() operator is implemented by applying the following differentiable q-norm (projection function):

$$\rho_i = \left(\sum_{j \in \Omega_k} d_j^q \right)^{\frac{1}{q}} \quad \text{with} \quad q > 0 \tag{2}$$

which makes the pseudo-density ρ_i to assume the largest value of variables d_j located in the Ω_k region, as described in Fig. 5.

Thus, variables d_j are converted into pseudo-densities ρ_i, for each iteration of the optimization problem, which summation is calculated to evaluate the objective function and volume constraint values. Then, the sensitivity values are calculated and a new set of optimized design variables d_j is obtained. It is necessary to assure that the volume constraint will be maintained, even when the projection domains of each variable are alternated. This procedure is repeated at each iteration of the optimization process until convergence is found.

4.3. Sensitivity analysis

As mentioned in the previous Section, it is possible to calculate pseudo-density ρ_i as a function of design variables d_j. Considering an objective function given by $\Theta \equiv \Theta(\rho(d))$, the sensitivities in relation to variables d_j are calculated by considering the pseudo-densities composed under the influence of the related domain Ω_k. Thus, any change in variables d_j, belonging to domain Ω_k, modifies the pseudo-density value ρ_i. Hence, the sensitivity of function Θ is calculated as follows [14]:

$$\frac{\partial \Theta(\rho(d_j))}{\partial d_j} = \sum_{i \in \Omega} \frac{\partial \Theta}{\partial \rho_i} \frac{\partial \rho_i}{\partial d_j} \tag{3}$$

where Ω is the entire domain. The sensitivity defined in Eq. (3) are obtained by the adjoint method [1]. Considering Eq. (2), the derivative of the pseudo-density ρ_i can be calculated analytically with respect to design variables d_j by:

$$\frac{\partial \rho_i}{\partial d_j} = d_j^{q-1} \left(\sum_{j \in \Omega_k} d_j^q \right)^{\frac{1}{q}-1} \quad \text{with} \quad q > 0 \tag{4}$$

5. Manufacturing constraints

There are several processes for manufacturing parts of structures and machines [17]. Each process has its own features and characteristics. Among the most well-known processes, we can mention: casting, forging, turning, milling, drilling, extrusion, forming, rolling, electrical discharge machining, laser-cutting, and others. For all these processes, internal holes should be avoided because it is not practical from an engineering point of view.

5.1. Casting

Casting is one of the oldest manufacturing techniques; however, it is still one of the most adopted in practice for manufacturing machine parts of various shapes and sizes. The technique consists in filling the form-work with liquid metal that conforms to the desired shape so that the actual component is obtained upon solidification by cooling the metal.

In order to achieve a simple casting process, the holes must be aligned along a single direction coinciding with the direction of the form-work removal. Holes in other directions, if existent, should obey the criteria illustrated in Fig. 6a. The conditions illustrated in Fig. 6b and Fig. 6c cannot be executed by means of simple casting process; however, they can be executed by means of lost-wax casting process. In this case, the form-work is made of wax and subsequently destroyed in order to extract the actual part.

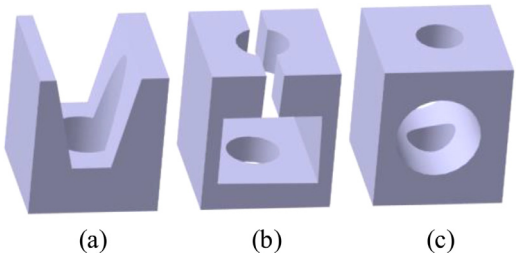

Fig. 6. (a) Acceptable hole associated with traditional casting operation; (b) and (c) acceptable holes in the "lost-wax" process.

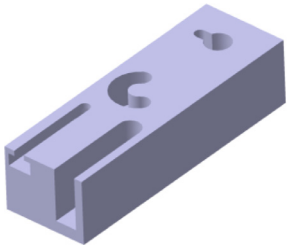

Fig. 7. Component manufactured by the milling process.

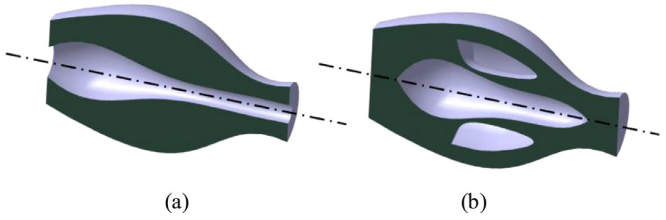

Fig. 8. (a) Component can be manufactured by the turning process; (b) internal features that cannot be manufactured by the turning process.

5.2. Milling

Milling consists in removing material by using a rotating tool while the basic part being manufactured remains fixed on a strong platform. This process allows the material to be removed in different directions with, most commonly, a rotating tool of cylindrical shape. The process may be used to cut parts with hole dimensions that are either equal or greater than the rotating tool radius, which allows detailing as illustrated in Fig. 7.

Milled parts can have cuts of different shapes because the tool can access the entire part domain. However, in general, it is not practical to produce deep cuts when there is no immediate access to the milling tool or other interior cuts without external access.

5.3. Turning

Turning is the most basic manufacturing process, in which a part is rotated while it is axisymmetrically machined by a cutting tool. It is very often used for producing a wide variety of round shape parts, such as shafts, spindles, pins, tubes, and anything that essentially has axisymmetric shapes. The component must be axisymmetric, as shown in Fig. 8a. Holes are allowed if axisymmetric and present some connection with the exterior part; therefore, internal holes cannot occur (Fig. 8b).

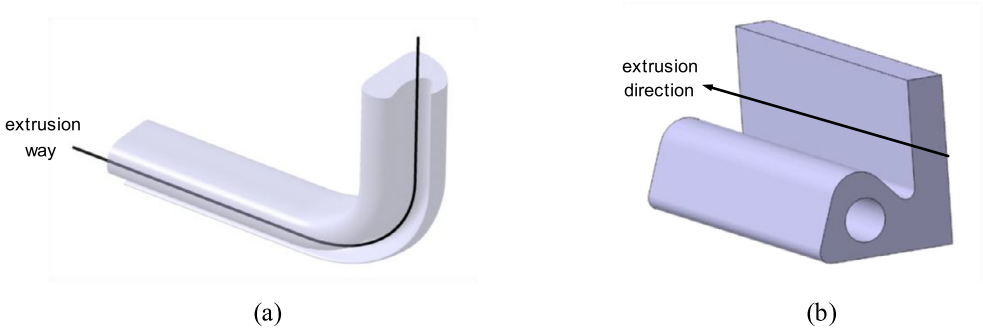

Fig. 9. Examples of extruded components: (a) solid cross-section; (b) hollow cross-section.

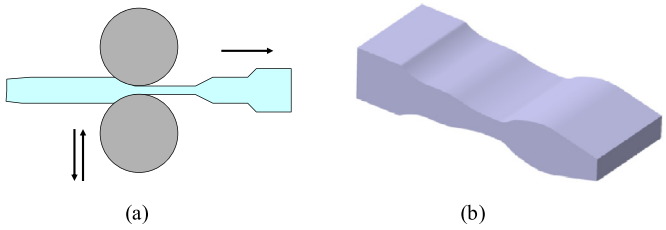

Fig. 10. (a) Scheme of the rolling process; (b) part manufactured by the rolling process.

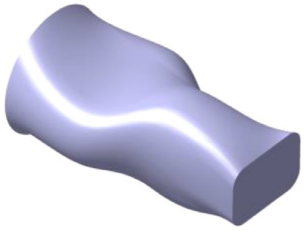

Fig. 11. Part component manufactured by the forging process.

5.4. Extrusion

In the extrusion manufacturing process, a warm cylindrical billet is forced through a die containing a defined profile, producing a bar lengthened with constant cross-section along the extrusion direction. In general, this manufacturing process is used for generating solid or hollow cross-sections of a wide variety of straight or curved structural beams and rails, as illustrated in Fig. 9.

5.5. Rolling

Rolling is the manufacturing process for reducing the thickness of a long work-piece by compression loads applied through a set of rolls, as illustrated in Fig. 10a. Symmetrical parts are obtained through this manufacturing process. From the smooth curvature radius, printed by the radius of the roll, a constant transversal cross-section is produced along the manufacturing process.

Rolling is carried out at elevated temperatures (hot rolling) or at ambient temperature (cold rolling), providing similar geometrical results in both cases. The choice between both processes is associated to the enhanced material properties of the rolled part, such as strength and hardness. Symmetry constraints for unique cross-section and smooth curvature radius are employed to construct a part by rolling process. Fig. 10b shows a feasible part to be manufactured by the rolling process.

5.6. Forging

In forging, a work-piece is shaped by sequential beats or, depending on the case, by a beat applied through various dies and tooling. In simple forging process, a solid work-piece with the desired size is formed by flat dies, in which material spreading occurs. Very often, it only aims to provide better characteristics for the material, rather than obtaining the finished shape of the component. In other forging process, a work-piece takes the shape of the die cavity while being forged between two shaped dies. In this case, the metal flow is conducted in a die to acquire a form very close to the expected part shape.

Forging can occur at elevated temperatures or at ambient temperature and the forged parts have the same characteristics in both cases, such as the non-existence of abrupt curvature radius changes or holes in any direction, as can be seen in Fig. 11.

A forged part is usually subjected to additional finishing processes to obtain accurate dimensions and finished surface in some regions. However, the nature of the forged part does not usually suffer great changes. Thus, it is important to obtain results that meet these constraints.

6. Numerical implementation

To implement the previously described manufacturing constraints in a topology optimization framework, different constraints are developed based on a unified projection-based approach. Thus, some aspects regarding the implementation of these constraints by efficiently combining the considered projection with the domain mapping technique are described in this Section. Details of the following constraints are given: minimum member size, minimum hole size, symmetry, extrusion, pattern repetition, turning, casting, forging, and rolling. Moreover, the implementation of the topology optimization problem, including the projection technique, is described.

6.1. Minimum member size

Minimum member size is one the most well-known and utilized constraint for controlling the minimum length scale of structural members, which has been implemented in many works [13,14,24,25], aiming at solving the long-standing checkerboard problem, the non-uniqueness of solutions, and the gray scale. This constraint forces a defined area, which must contain a maximum pseudo-density value, upon each element of the discretized domain.

As shown in Fig. 12, pseudo-densities are mapped such that each variable d_j must represent its equivalent position in a pseudo-density domain (ρ), represented by a circular region (Ω_k) with a defined radius (R) around the element. Each element in the Ω_k domain influences the sensitivity of the variable (d_j); however, as the

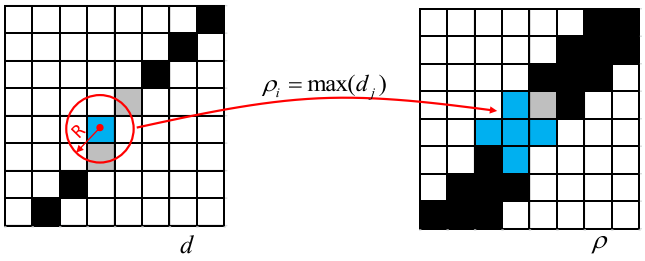

Fig. 12. Projection scheme for minimum member size constraint.

projection function of Eq. (2) is applied, the value closer to the largest value of the design variable (d_j) is obtained and projected upon each pseudo-density ρ_i, when mapping is performed.

Hence, elements having design variable d_j values close to 1 assume a circular area made of pseudo-density values equal to 1, overlapping possible intermediate areas made of elements with pseudo-density values between 0 and 1.

6.2. Minimum hole size

Although the minimum member size is an efficient constraint to solve the main numerical problems of topology optimization, it generates solutions as shown in Fig. 13a, in which the distance between minimum members is very small, making the construction of these members extremely difficult or unfeasible.

Thus, the minimum hole size constraint controls the distance between members, allowing generating a space required for a cutting tool to work between these members. This constraint has been implemented in other works [13,25], and it can control the minimum size of possible holes in the solution. However, it can also indirectly control the number of members, driving the solution toward a unique member feature.

In this work, its numerical implementation is analogous to the minimum member size described in Section 5.1. The mapping variable is the same as before (Fig. 4); however, the projection scheme uses an opposite projection function, which makes the pseudo-density ρ_i to assume a value close to the smallest value of the design variable d_j projected on Ω_k, that is:

$$\rho_i = \left(\sum_{j \in \Omega_k} d_j^q \right)^{\frac{1}{q}} \quad \text{with} \quad q < 0 \tag{5}$$

Although this constraint limits the minimum size of holes for the solution, one must be careful when applying minimum hole size constraint combined with the minimum member size constraint, since both criteria are contradictory [25]. The work of Guest [26] proposes a scheme to combine both constraints by projection [13]. However, the examples shown ahead consider the two constraints applied separately herein.

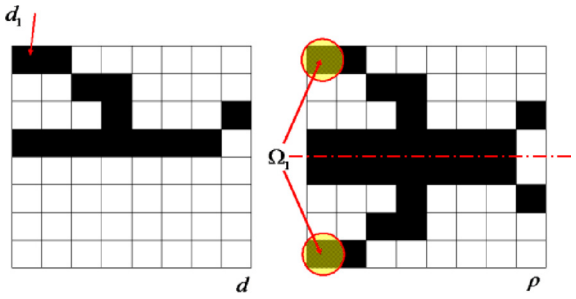

Fig. 14. Mapping used for symmetry constraint.

6.3. Symmetry

Although symmetry constraint may not be considered a manufacturing constraint, it is necessary for other constraints, such as forging, rolling, and extrusion. Symmetry constraint provides results that assure symmetry behavior independently of the loading condition. Fig. 14 illustrates a symmetry constraint in the XZ plane. Elements of the domain Ω_i having the opposite coordinate geometric centers along the direction normal to the symmetry plane are considered. The center distances are always compared with a 1% tolerance of dimension of the largest existent element in the model in a considered direction. When more than one symmetry plane is considered, vectors are independently constructed for each of the three planes (XY, XZ, and YZ). Then, the symmetry operation is sequentially applied to the model to mirror its region until the domain total volume is rebuilt [25]. However, the sensitivity in relation to each design variable must be multiplied by the number of symmetry planes.

6.4. Pattern repetition

Pattern repetition constraint generates domains with repeated cells in a controlled manner. It can be applied to either induce shape repetitions inside a continuous domain, driving equally all patterns by mimicking the material microstructure configuration, or to assure that different regions subjected to different load conditions should assume the same topology for all situations.

If only "continuous" domain (Fig. 15) and repeated shape regarding the same coordinate systems are considered, the variables are mapped by adopting the whole domain as reference, and by dividing the structure in three coordinate directions (X, Y, Z), accord-

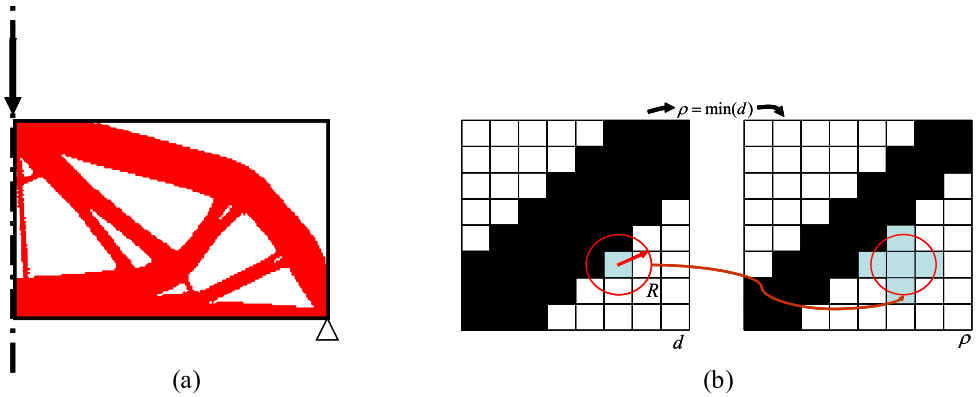

Fig. 13. (a) Example of solution with small holes between structural members; (b) minimum hole size scheme.

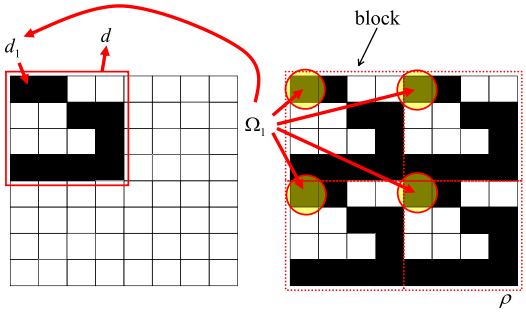

Fig. 15. Mapping for pattern repetition constraint.

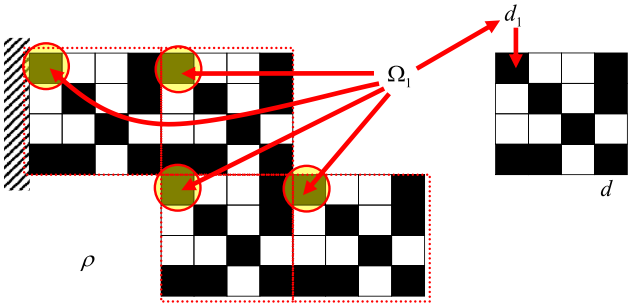

Fig. 16. Mapping of pattern repetition constraint in non-continuous domains.

ing with user requirments. A reference element is then defined inside each block by knowing the number of elements at each direction. Moreover, all the other elements form this block are included in the Ω_k domain represented by d_j, considering its position in relation to the reference element [25]. However, the sensitivity in relation to each design variable must be multiplied by the number of repeated patterns.

Otherwise, if "non-continuous" domains (e.g. Fig. 16) are considered, the FE model must be built by indicating what volume is defined for a block, and where the origins of all the other existent blocks are localized, as well as which directions of the local coordinates system must be used for mapping this block.

Projection function of Eq. (2) is not necessary for projecting design variables d_j since there is no superposition of domains. Thus, the projection is carried out by directly mapping the design variable values to corresponding pseudo-density values. Moreover, the pattern repetition constraint uses the relative position among elements to perform the domain mapping; thus, the element size is not important. However, the FE mesh must be structured, and the number of elements must be repeated by patterns. Domains with different scale factors are allowed; however, a geometric mapping

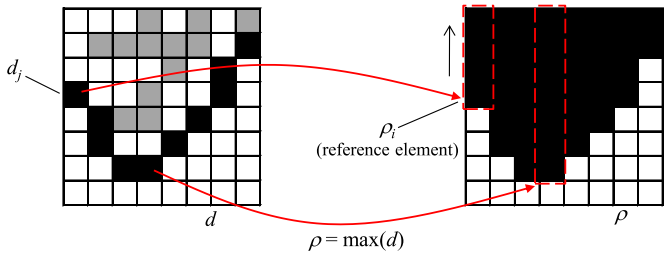

Fig. 18. Reference direction defined for casting manufacturing constraint.

will be necessary for the pattern repetition constraint in order to obtain equal patterns for different discretized meshes.

6.5. Extrusion

Extrusion aims to guarantee that only a cross section is repeated throughout the domain. Thus, a cross section area of the model is defined as design variables (d_j), which should represent all the elements contained in an extrusion direction. As shown in Fig. 17, the Ω_k domain is mapped along the direction of a coordinate axis normal to a reference plane. Then, all the elements contained in the extrusion direction are included in the design domain. Due to the structured mesh, the number of finite elements at each Ω_k domain is always constant, indicating that all sections have the same number of elements, yet they may have different aspect ratios (tapered domain).

The extrusion manufacturing constraint uses the projection technique to turn the design variable d_j into equivalent pseudo-densities. However, as in the pattern repetition constraints, projection functions of Eqs. (2) or (5) are not needed here, either. Domain superposition does not occur; thus, mapping is applied only to transfer the values of design variable d_j to finite element pseudo-densities (that belong to Ω_k domain). However, the sensitivity in relation to each design variable must be multiplied by the number of element layers in the direction normal to the reference plane.

6.6. Casting

The casting manufacturing constraint aims to find a solution in which the holes are aligned along a single direction. This constraint defines a set of design variables (d_j) such that each of these variables represents a reference element in the pseudo-density domain (ρ), whose value is reproduced to all the element pseudo-densities positioned below this reference element (ρ_i), as shown in Fig. 18. Thus, a direction must be defined as reference to the casting manufacturing constraint. As in the minimum member size constraint,

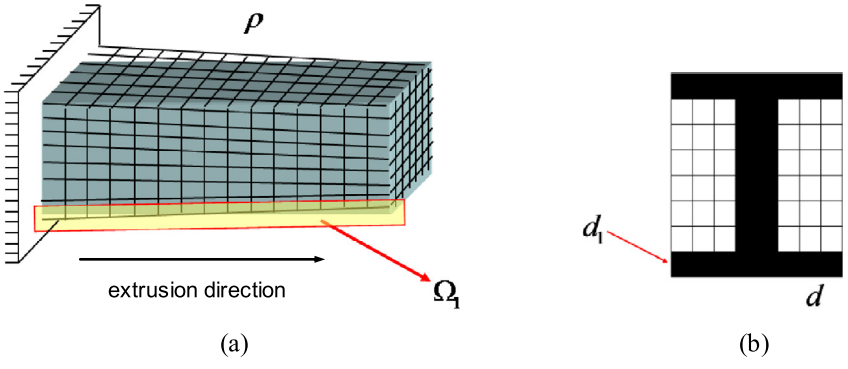

Fig. 17. Extrusion constraint: (a) tapered design domain; (b) design variables d_j (cross section area).

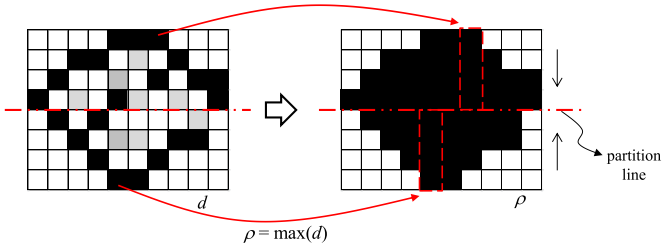

Fig. 19. Mapping and projection techniques applied to implement the "two-parts" casting manufacturing constraint.

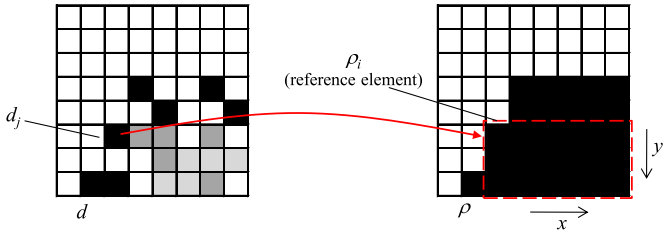

Fig. 21. Rectangular areas defined by the x and y reference directions in the forging constraint.

there is a superposition of pseudo-density values; thus, the projection function of Eq. (2) is applied to bring the value closer to the largest value among them.

This variable mapping technique follows the procedure depicted in Fig. 4 and allows elements to have at least the same pseudo-density value as the reference element. Nevertheless, it generates a plane face in the solution, which it is defined as a top side (Fig. 18). In other words, this solution allows obtaining a casting mold with a plane surface. To obtain a more general solution, allowing a "two-parts" model, a set of design variables (d_j) is implemented, as illustrated in Fig. 19. The mapping of this set of variables is performed in the same way depicted in Fig. 18; however, generating one solution as bottom side and another as top side (see Fig. 19). Then, now there are two opposite mapping variables which produce two solutions (casting molds) for the optimization problem, each one from a reference partition face that defines the division of the two casting molds. To accomplish a unique solution, these two solutions are obtained by the projection function of Eq. (3) to ensure the required casting design. Thus, the final pseudo-density always assumes the largest possible pseudo-density value found in this solution.

6.7. Turning

The turning constraint aims to find a solution in an axissymetric domain in which holes must have some connection with the external part. In this sense, its implementation is quite similar to the idea of the casting constraint implementation. A set of design variables d are implemented and the reference direction is defined to follow longitudinal (+X, –X) and radial (Z+, –Z) directions. Four mappings of these variables are performed in the same way, with reference faces located on the right (+X), left (–X), top (–Z), and down (Z+) sides of the pseudo-density domains, as illustrated in Fig. 20.

As in the casting constraint, there is a superposition of the pseudo-density domains; the projection functions of Eqs. (2) and (5) are thus applied to reach values closer to the largest or smallest value among them, respectively. This procedure follows the mapping scheme depicted in Fig. 4, and it is repeated at each iteration of the optimization process until convergence is found.

6.8. Forging

As in the turning constraint, forging constraint follows the mapping procedure depicted in Fig. 4, and uses four sets of design variables (d_j), applying four mapped domains in total. Initially, a reference plane is defined, which is utilized to produce the mapped domains. In the next step, the domains of each element layers are created following the parallel direction of this reference plane.

Similar to the casting constraint, each design variable (d_j) represents a reference element in the pseudo-density domain (ρ), whose value is reproduced for all the element pseudo-densities located between the x and y axis directions from the reference element (ρ_i), as shown in Fig. 21. Thus, a rectangle area is created beginning at the reference element and spreading to the end of the pseudo-density domain, in a specified quadrant of the mapped domain (see Fig. 21).

In this case, four domain variable mappings are carried out, as depicted in Fig. 22, where each one considers a different quadrant from the reference elements. The sensitivity of each mapped domain is calculated separately, as the problem is solved. Consequently, a solution is achieved for the set of variables d of each of the four mapped domains. As in casting constraint, the projection function of Eq. (5) is applied to obtain the intersection of the mapped domains and to find the final solution at each iteration. Then, these results are used for the sensitivity calculation of the next iteration.

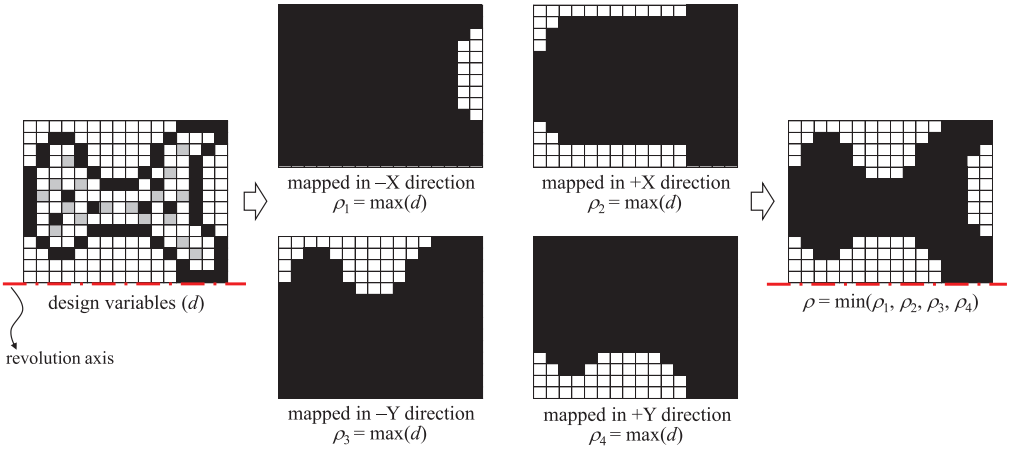

Fig. 20. Mapping technique applied to implement the turning manufacturing constraint.

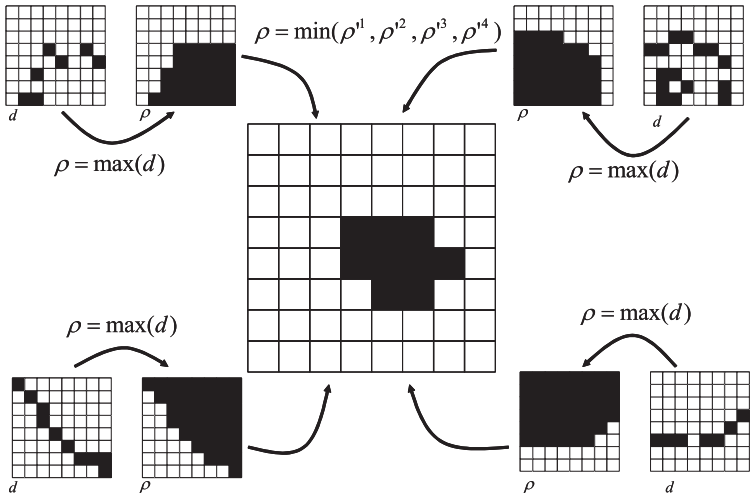

Fig. 22. Mapping scheme used for implementing forging constraint.

6.9. Rolling

The rolling constraint is created by using the other constraints previously described. In this case, the casting constraint is used by considering only a reference plane located at its center together with a symmetry constraint, allowing that the two halves, obtained by casting constraint, to be identical. The smoothness of a curvature radius is achieved by using the minimum member size, followed by extrusion constraint which should be applied in a direction transversal to the rolling direction to achieve the final solution.

6.10. Topology optimization procedure

The performance of the proposed manufacturing constraints is assessed by the computational implementation of the following minimum compliance problem:

$$\begin{aligned} &\underset{0<\mathbf{d}\leq 1}{\text{minimize}} : \mathrm{C}(\boldsymbol{\rho}) = \mathbf{f}^T\mathbf{u} \\ &\text{subject to: } \boldsymbol{\rho} = f(\mathbf{d}) \\ &\qquad \mathbf{K}(\boldsymbol{\rho})\mathbf{u} = \mathbf{f} \\ &\qquad \sum_{i=1}^{N} \rho_i v_i \leq V \end{aligned} \tag{6}$$

where $\mathrm{C}(\boldsymbol{\rho})$ is the objective function representing the compliance, **u** is the global displacement vector, which depends on design variables **d, K** is the global stiffness matrix, **f** is the global load vector, V is the volume constraint, v_i is the volume of each element, and N is the number of elements of the domain. To avoid numerical problems a very small value (10^{-6}), instead of zero, is adopted for the minimum value of the design variables.

This optimization problem is solved by using the Method of Moving Asymptotes (MMA) [19] through an iterative algorithm shown in Fig. 23, which depicts the topology optimization implementation containing the projection technique.

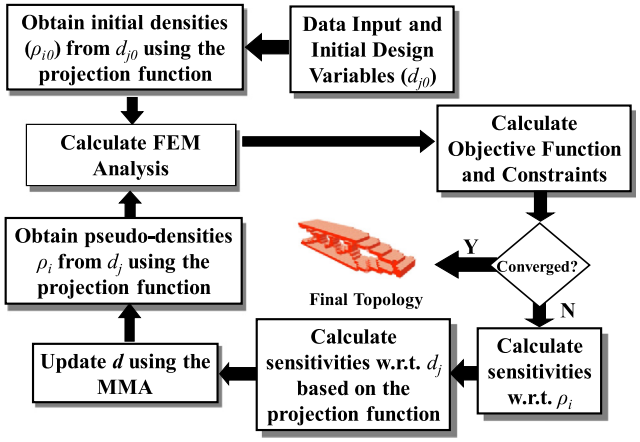

Fig. 23. Flowchart of the topology optimization procedure.

7. Results

For all the examples in this section, the material considered in numerical models has $E = 100$ (Young's modulus) and $\nu = 0.3$ (Poisson's ratio), and the applied load is considered equal to 100. Consistent units are employed. The design domains are discretized by using the traditional bilinear plane elements (2D domains) and trilinear solid elements (3D domains) [20]. The boundary and load conditions are depicted in the figures of the examples. The following results use at least one manufacturing constraint, and the minimum member size constraint is applied to all the obtained solutions, as depicted in Fig. 1, except for solutions employing the minimum hole size constraint. For comparison, the optimized compliance value (C^*) achieved for each topology optimization results are indicated in the caption of the most figures presented ahead.

7.1. Minimum member size constraint

The minimum member size constraint drives the implemented algorithm to search for a solution with a minimum length scale for the structural members, as required by the design. Fig. 24 shows the relation between variables d and the final solution obtained for the pseudo-densities ρ, by considering the minimum member radius (R) equal to 0.5.

Firstly, it is noticed this result (Fig. 24) is free for checkerboard problem, which would not be achieved in that way with no minimum member size constraint. A minimum compliance value ($\mathrm{C}*$) equal to 73.0 is achieved herein. Moreover, this constraint does not generate new members in the solution. Nevertheless, the minimum member size can control the number of possible members in the solution. For instance, Fig. 25 shows two different solutions for the same problem; however, the minimum member radius (R) is changed. This problem is solved by using a 50% volume constraint to the domain discretized into 5000 elements.

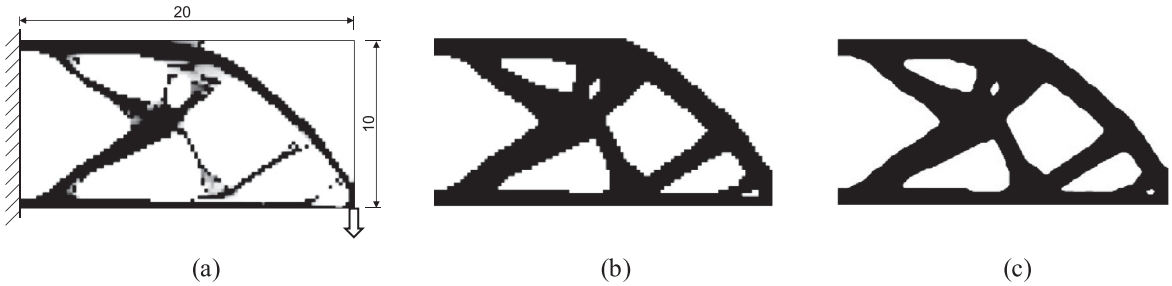

Fig. 24. Results obtained by using 50% volume constraint to the domain discretized into 5000 elements: (a) design variable d; (b) pseudo-density ρ; (c) post-processed view of the result (pseudo-density).

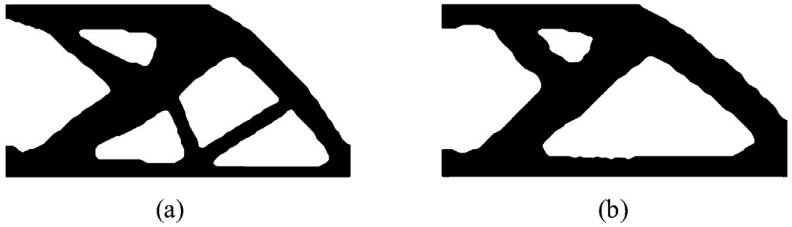

Fig. 25. Post-processed view of the result from using different radius for the minimum length scale of structural members: (a) R = 0.3 (C∗ = 73.3); (b) R = 1.0 (C∗ = 81.4).

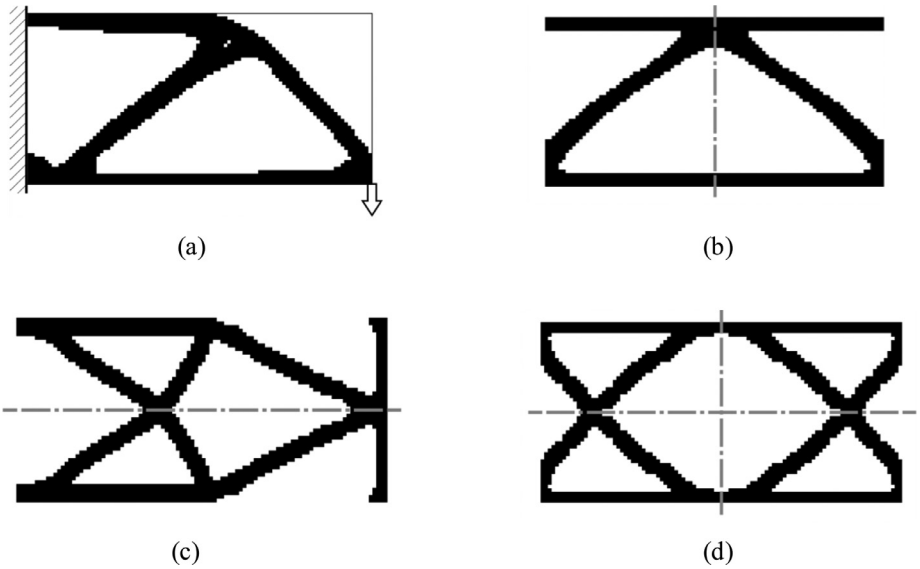

Fig. 26. A comparison between results obtained by using the minimum member size constraint: (a) without symmetry constraint (C∗ = 127.6); (b) with symmetry constraint in the vertical plane (C∗ = 216.0); (c) with symmetry constraint in the horizontal plane (C∗ = 153.8); (d) with symmetry constraint in the two planes simultaneously (C∗ = 335.1).

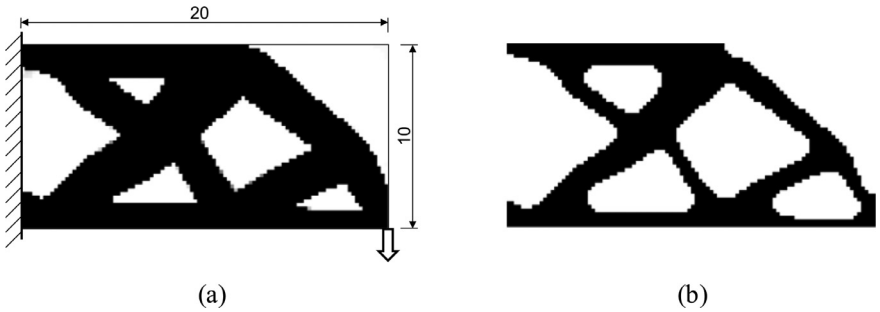

Fig. 27. Results obtained by using a 40% volume constraint to the domain discretized into 5000 elements, and by considering the minimum radius size of holes (R) equal to 0.7: (a) design variable d; (b) pseudo-density ρ.

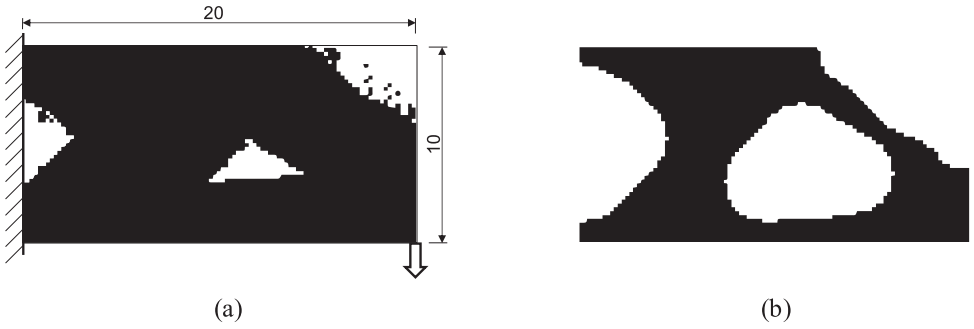

Fig. 28. Results obtained by using a 40% volume constraint to the domain discretized into 5000 elements, and by considering R = 2.0: (a) design variable d; (b) pseudo-density ρ.

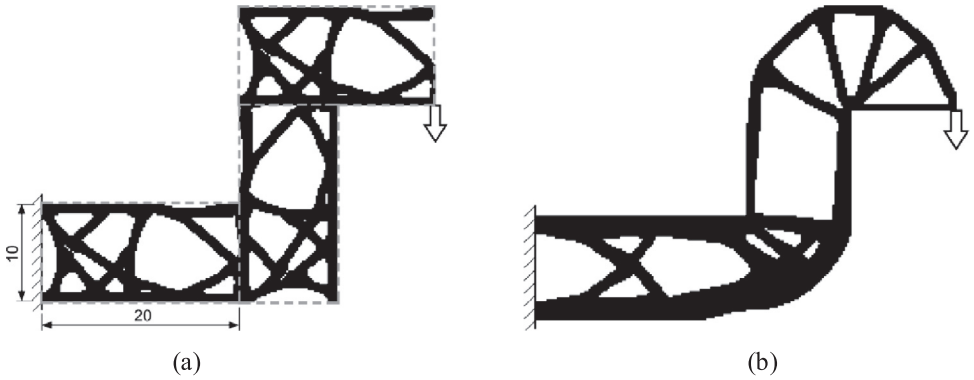

Fig. 29. Results obtained by using a 50% volume constraint to the domain discretized into 15,000 elements: (a) with pattern repetition constraint ($C* = 0.68$); (b) without pattern repetition constraint ($C* = 0.43$).

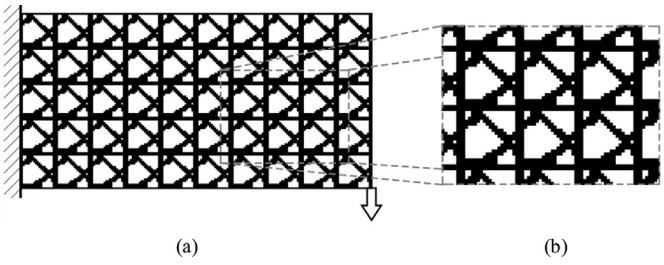

Fig. 30. Results obtained by using 10×5 patterns and by considering the whole domain discretized into 20,000 elements: (a) pattern repetition applied to generate a basic cell of the composite material; (b) amplified cell detail.

A symmetry constraint can be applied to the previous results. Fig. 26 shows a comparison between results without symmetry constraint (Fig. 26a) and others achieved by considering symmetry constraint regarding a vertical plane (Fig. 26b), a horizontal plane (Fig. 26c), and two planes simultaneously (Fig. 26d). These results are obtained by using the minimum member radius (R) equal to 0.5, and by considering a 30% volume constraint to the domain discretized into 5000 elements. These results are verified to be significantly different according to the symmetry constraint applied. Symmetry constraint completely changes the solution.

7.2. Minimum hole size constraint

In this case, this constraint provides an opposite behavior in relation to the minimum member size, that is, the domain variables (d) have larger scale members than the solution given by the domain pseudo-densities (ρ), as can be seen in the example of Fig. 27. By using minimum hole size, new members are not generated in the solution, as occurs by using the minimum member size (presented in the previous Section). Moreover, as the mini-

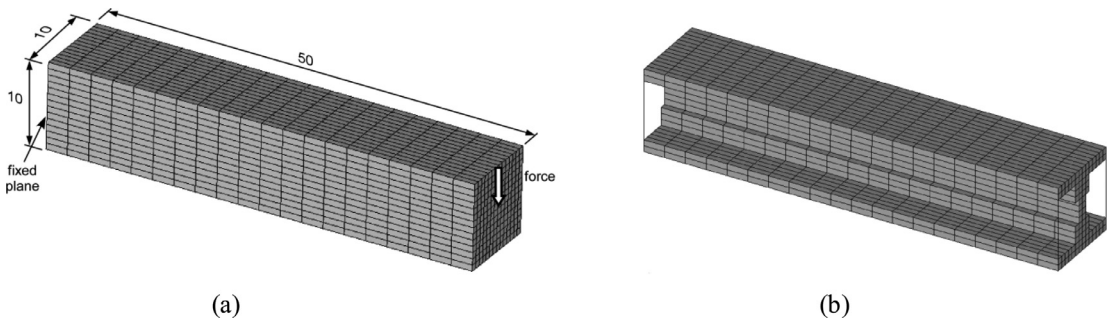

Fig. 31. Result obtained by using the extrusion constraint: (a) design domain discretized into 3920 elements; (b) beam profile "I" obtained by using a 30% volume constraint ($C^* = 74.3$).

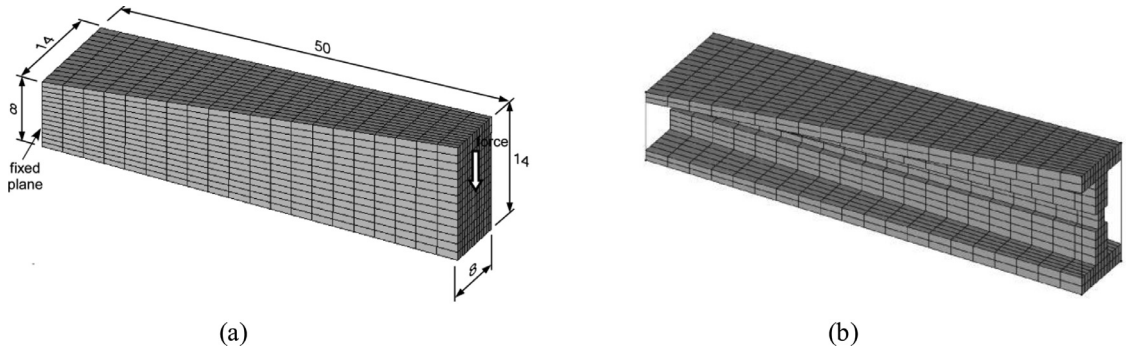

Fig. 32. Result obtained by using the extrusion constraint: (a) tapered design domain discretized into 3920 elements; (b) cantilever beam obtained by using a 30% volume constraint ($C* = 75.9$).

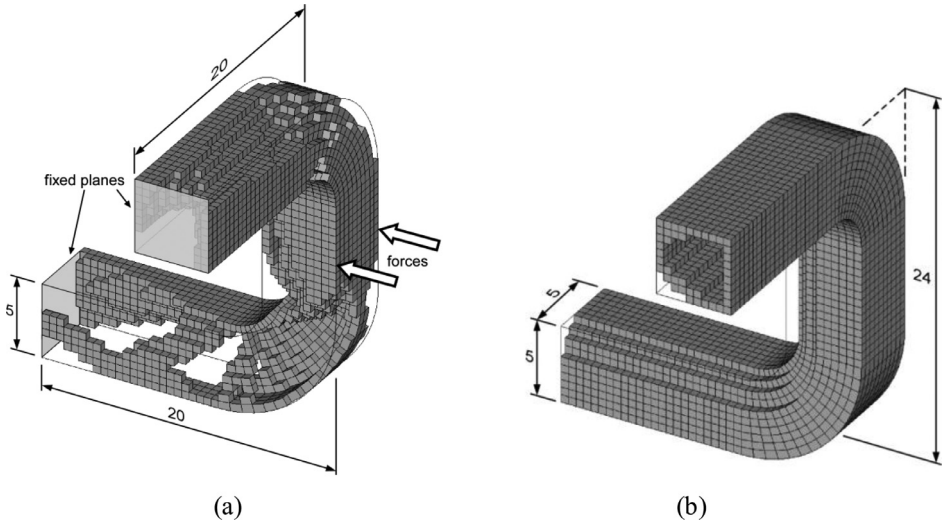

Fig. 33. Results obtained with 50% volume constraint: (a) without extrusion constraint ($C* = 58.7$); (b) with extrusion constraint ($C* = 62.7$).

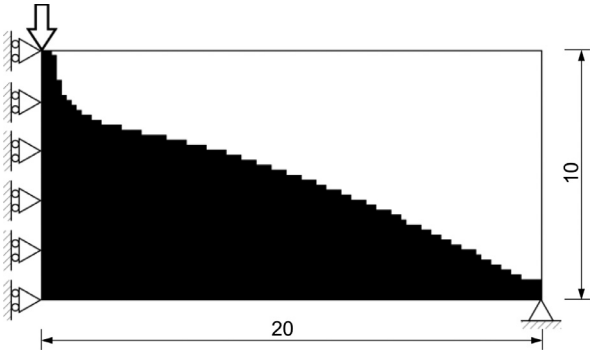

Fig. 34. Solution obtained by considering one way casting, and a 50% volume constraint to the domain discretized into 5000 elements ($C* = 95.2$).

mum hole radius (R) of this constraint is increased, very different results are obtained (Fig. 28).

Differently from the results obtained by controlling the minimum length scale of the structural members through the minimum member size constraint (see Fig. 25), here the algorithm must remove mass of elements needed to include holes in existing spaces. Then, it groups all holes in the same space, generating a unique large hole, as can be seen in Fig. 28. By increasing the minimum hole radius (R) a small number of members in the solution is provided. A minimum compliance values ($C*$) equal to 102.2 and 141.3 are achieved for the results shown in Fig. 27 and Fig. 28, respectively.

7.3. Pattern repetition constraint

Fig. 29 illustrates the result obtained by using a pattern repetition constraint, by considering the minimum member radius (R) equal to 0.5. Thus, the mass distribution is more uniform in the solution, instead of accumulating in only one region of the domain as occurs in Fig. 29b.

This constraint can create a basic cell, which can be repeated several times into a domain to generate a structure (see Fig. 29a). Thus, it can be applied to design structures based on composite materials. In this case, a pattern repetition constraint is specified that generates a periodic matrix of the unit cells, each one representing a microstructure, as illustrated in Fig. 30.

Here, the appearance of large gray scale regions is more critical, as several cells and small relevance regions into the domain need to be filled with mass. Thus, the volume constraint must be increased until a satisfactory solution can be found.

7.4. Extrusion manufacturing constraint

Beam profile "I" can be demonstrated to be the best solution for a cantilever beam problem by using the extrusion constraint (see Fig. 31), even considering any cross-section aspect ratio (tapered domain), as illustrated in Fig. 32. In these solutions, another highlighted characteristic is the fact that all solutions are symmetric. Although symmetrical solution should be expected, due to symmetrical boundary conditions, this should not occur naturally,

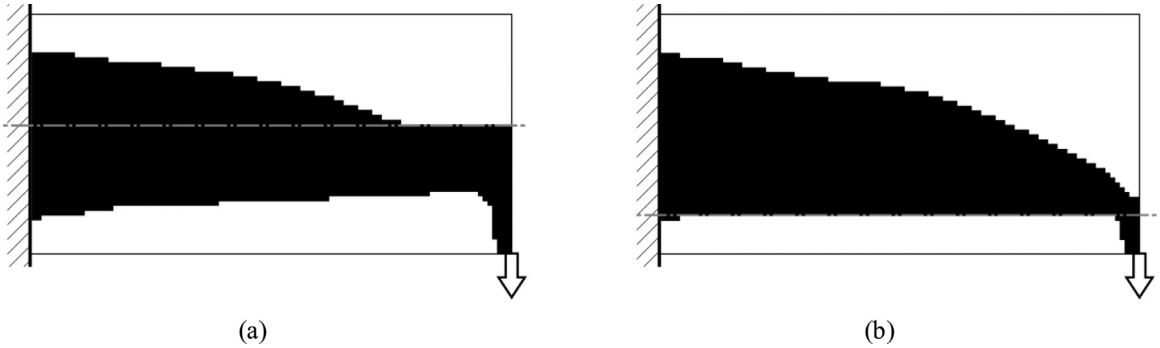

Fig. 35. Result obtained by considering two molds casting, and a 50% volume constraint to the domain discretized by 5000 elements: (a) two molds with the same aspect ratio (domain is divided into two symmetric parts, $C* = 237.7$); (b) two molds with different aspect ratio (bottom part corresponds to 20% of total the domain height, $C* = 204.7$).

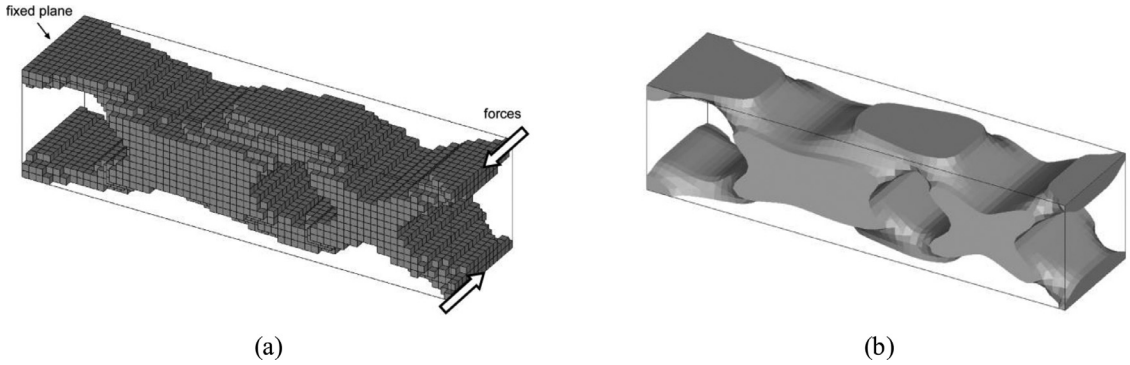

Fig. 36. Casting manufacturing constraint applied to a beam under torsion load, by considering the domain discretized into 16,384 elements ($16 \times 16 \times 64$): (a) result obtained by using a 50% volume constraint ($C* = 0.642$); (b) post-processed view.

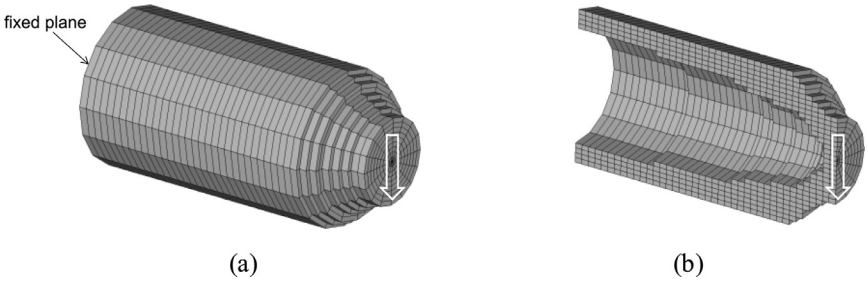

Fig. 37. Solution obtained by considering turning constraint, and by using a 50% volume constraint to the domain subjected to a single load ($C* = 0.951$): (a) external view; (a) section view.

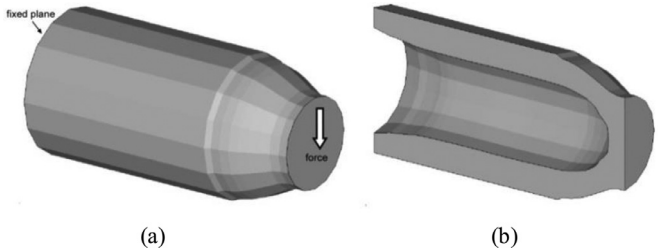

Fig. 38. Post-processed view of the result achieved by using turning constraint: (a) view of the result shown in Fig. 37; (b) section view of the result.

since the algorithm employed for solving numerically the FEM linear system (the conjugated gradient method, in this case) produces truncation errors. However, the projection technique used for extrusion constraint reduces this effect, giving a natural symmetric solution.

Extrusion constraint, implemented following a structured mesh, can also be applied to obtain a continuum-curved structures, such as a tube. Fig. 33 shows a comparison between results with extrusion constraint (Fig. 33b) and without it (Fig. 33a) obtained by using a 50% volume constraint to the domain discretized into 9400 elements. In this example, the result obtained with the extrusion constraint has optimized compliance value ($C*$) only 6.8% larger than the results obtained without this constraint (see Fig. 33). It is noticed how manufacturing of a part can be simplified by using extrusion constraint.

7.5. Casting manufacturing constraint

Fig. 34 illustrates a solution obtained by considering one way casting, in which a simple load condition creates a solid shape. Moreover, to allow for two-mold casting constraints, two mappings must be run considering opposite directions, and a reference plane that divides the domain into two parts (molds), which may be symmetric or not, as illustrated in Fig. 35.

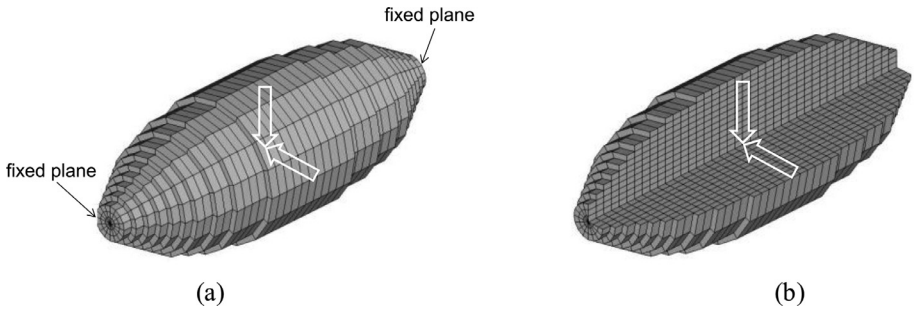

Fig. 39. Solution obtained by considering turning constraint, and by using a 50% volume constraint to the domain subjected to two loads ($C* = 0.996$): (a) external view; (a) section view.

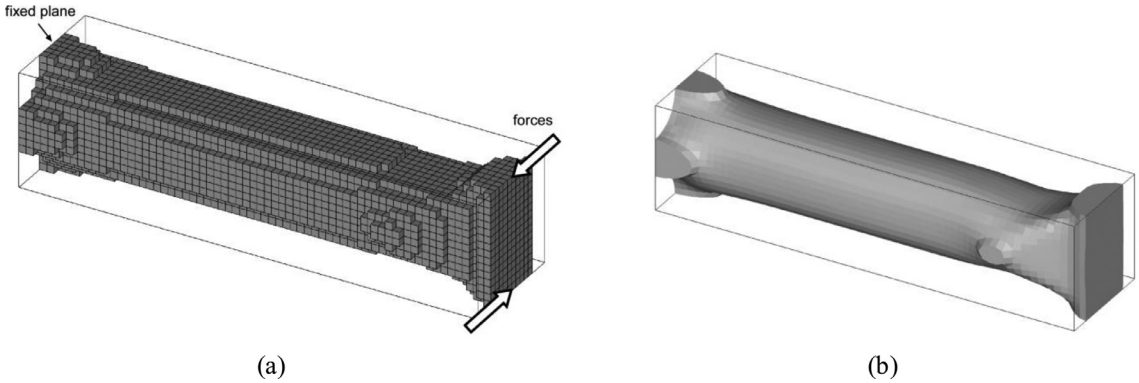

Fig. 40. Forging constraint and minimum member size applied to a clamped beam under torsion, by considering the domain discretized into 16,384 elements ($16 \times 16 \times 64$): (a) result obtained by using 30% volume constraint ($C* = 0.817$); (b) post-processed view of the result.

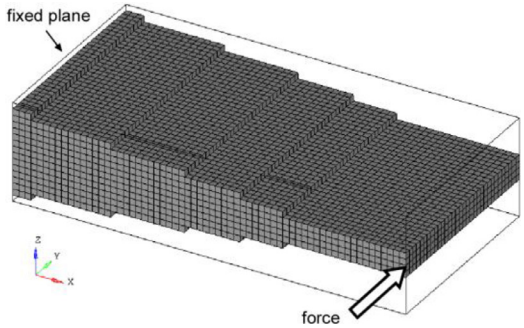

Fig. 41. Result obtained by using rolling constraint, considering the domain discretized into 32,768 elements ($16 \times 32 \times 64$) and using 50% volume constraint.

Fig. 36 shows the result obtained for a tridimensional (3D) clamped beam under a torsion load. This solution is not intuitive, and the standard "X" solid beam is determined, which meets the construction requirements of the casting manufacturing process. Here, the optimized compliance value ($C*$) obtained with the manufacturing casting constraint is 43.6% larger than the compliance value obtained without this constraint.

A post-processed view (Fig. 36b) is performed in a CAD software to illustrate a better image of the topology optimization result (Fig. 36a). For all the examples presented herein, this post-processing is carried out after the last iteration of the optimization process, that is, when the final solution was already obtained.

The projection scheme, adopted in the casting manufacturing constraint, increases the stability of the numerical method of the implemented algorithm by reducing the rounding errors. Large gray scale region could appear by using the casting manufacturing constraint, since small important regions should necessarily have mass. Here, increasing the penalization factor of gray scales is not enough to solve this problem. In this case, the volume constraint must also be increased until a satisfactory solution is found.

7.6. Turning manufacturing constraint

The next examples illustrate the results obtained by applying the turning constraint. A cylindrical domain, discretized into 16,384 elements, is considered. In the first example (Fig. 37), one end of the cylindrical domain is clamped (fixed face) and a single vertical load is applied to the opposite free end. In a second example (Fig. 39), both ends of the cylindrical domain are clamped (fixed planes) and one vertical and other horizontal loads are applied to the center of the symmetry axis.

Thus, when the turning constraint is applied, a cylindrical part, which can be machined axisymmetrically, is naturally obtained (see Fig. 37). As illustrated in the post-processed view of the result shown in Fig. 38b, axisymmetric holes are allowed when applying this constraint. However, for the example in Fig. 39 it is not allowed, since the formation of an internal hole would be nearly impossible to be manufactured by the turning process.

In this example, the result obtained with the turning constraint has optimized compliance value ($C*$) only 5.2% larger than the results obtained without this constraint.

7.7. Forging manufacturing constraint

Fig. 40 shows the solution obtained by using forging constraint applied to a clamped domain under torsion. It is free of holes, and it has a smooth radius generated by using the minimum member size simultaneously (see post-processed view in Fig. 40b). Here, the optimized compliance value ($C*$) obtained with the manufacturing forging constraint is 62.2% larger than the compliance value obtained without this constraint.

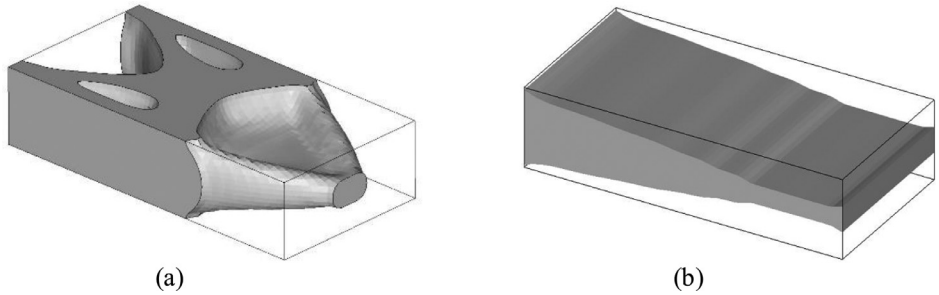

Fig. 42. Comparison between post-processing view of the results achieved: (a) without manufacturing constraint ($C* = 0.158$); (b) with rolling constraint ($C* = 0.235$).

7.8. Rolling manufacturing constraint

Rolling manufacturing constraint is performed by the superposition of some of the manufacturing constraints previously described. The superposition of constraints does not cause conflicts, and assures determination of the necessary requisites for the solution. Fig. 41 presents the result obtained by considering the minimum member size, symmetry, casting, and extrusion constraints, which are applied simultaneously to find a solution that provides all the necessary requisites for designing a part to be manufactured by using the rolling process.

Fig. 42 shows a post-processed view for comparison between results obtained without manufacturing constraint and with rolling manufacturing constraint for the example presented in Fig. 41. As can be seen, the optimized compliance value obtained with the rolling constraint is 48.7% larger than the compliance value obtained without this constraint. However, the result achieved without manufacturing constraint (Fig. 42a) has holes and features not allowed to be manufactured by the desired manufacturing technique (rolling).

8. Conclusions

Manufacturing constraints are able to limit the range of solutions to topology optimization problems. The implemented technique considers a domain of design variables and then projects these results in a pseudo-density domain to obtain the optimized solution. The relation between both domains is defined by the projection function and variable mappings according to each constraint of interest. This leads to a unified projection-based approach for implementing manufacturing constraints in topology optimization. The minimum member size, minimum hole size, symmetry, extrusion, pattern repetition, turning, casting, forging and rolling constraints have been implemented. These constraints illustrate the capability of the projection scheme to control the optimization solution without adding a large computational cost.

As expected, the introduction of the manufacturing constraints modifies the solution, affecting the minimum compliance values ($C*$) of the topology optimization results. The impact of the manufacturing constraints in the performance of the results depends on the kind of the manufacturing constraint applied. For example, the compliance value obtained with the extrusion constraint is 6.8% larger than the compliance value obtained without this constraint, while the result obtained with rolling constraint is 48.7%. Nevetheless, it is emphasized that the topology optimization results are obtained in accordance with requirements of the desired manufacturing constraint, which makes these results easier to be manufactured by the traditional manufacturing techniques.

The manufacturing constraints, such as extrusion, casting, forging, turning, and roling eventually request the increase of the penalization factor (p) and the material (volume constraint) because there is a trend of filling small relevance regions with material. Otherwise, large gray-scale regions (intermediate pseudo-densities) may appear.

The present approach makes room for extension to other constraints such as a minimum member size with variable radius along the domain, or along the optimization iterations, so that the solution can be geared toward the expected result. Moreover, extension of manufacturing constraints to plates and shells, including manufacturing processes besides the ones investigated herein (e.g. stamping and welding of thick plates), can lead to further developments in the field. Further developments in this area can also have an impact on industrial processes and successfully contribute to technology transfer.

Acknowledgements

The first and second authors thanks the São Paulo Research Foundation (FAPESP) for supporting him in his graduate studies, through the fellowship 2008/57086-6. The third author also thanks FAPESP for the financial support provided by research grant 2015/08316-2. The fourth author acknowledges support from the US National Science Foundation through grant CMMi 1321661. The last author is thankful for the financial support also received from the National Council for Research and Development (CNPq) under the grant 304121/2013-4. All the authors also acknowledge the support by CAPES. The authors also thank Krister Svanberg for providing the MMA optimizer code.

References

[1] Bendsøe MP, Sigmund O. Topology optimization: theory, methods and applications. Berlin: Springer-Verlag; 2003.
[2] Sigmund O. Morphology-based black and white filters for topology optimization. Struct Multidisc Optim 2007;33:401–24.
[3] Sigmund O, Petersson J. Numerical instabilities in topology optimization: a survey on procedures dealing with checkerboards, mesh-dependencies and local minima. Struct Multidisc Optim 1998;16(1):68–75.
[4] Zuo K-T, Chen L-P, Zhang Y-Q, Yang J. Manufacturing- and machining-based topology optimization. Int J Adv Manuf Technol 2006;27(5-6):531–6.
[5] Harzheim L, Graf G. A review of optimization of cast parts using topology optimization. II-topology optimization with manufacturing constraints. Struct Multidisc Optim 2006;31(5):388–99.
[6] Ishii K, Aomra S. Topology optimization for the extruded three dimensional structure with constant cross section. *JSME Int J Series* A 2004;47(2):198–206.
[7] Lia H, Li P, Gao L, Zhang L, Wu T. A level set method for topological shape optimization of 3D structures with extrusion constraints. Comput Methods Appl Mech Eng 2015;283:615–35.
[8] Gersborg AR, Andreasen CS. An explicit parameterization for casting constraints in gradient driven topology optimization. Struct Multidisc Optim 2011;44:875–81.
[9] Zhu J-H, Gu X-J, Zhang W-H, Beckers P. Structural design of aircraft skin stretch-forming die using topology optimization. J Comput Appl Math 2013;246:278–88.
[10] Sørensen SN, Lund E. Topology and thickness optimization of laminated composites including manufacturing constraints. Struct Multidisc Optim 2013;48:249–65.
[11] Wang F, Lazarov BS, Sigmund O. On projection methods, convergence and robust formulations in topology optimization. Struct Multidisc Optim 2011;43:767–84.

[12] Leary M, Merli L, Torti F, Mazur M, Brandt M. Optimal topology for additive manufacture: A method for enabling additive manufacture of support-free optimal structures. Mater Design 2014;63:678–90.
[13] Guest JK, Prevost JH, Belytschko T. Achieving minimum length scale in topology optimization using nodal design variables and projection functions. Int J Numer Methods Eng 2004;61(2):238–54.
[14] Le CH. Achieving minimum scale and design constraints in topology optimization: a new approach. University of Illinois at Urbana-Champaign (UIUC); 2006. MS Thesis.
[15] Del Prete A, Mazzotta D, Anglani A. Design optimization application in accordance with product and process requirements. Adv Eng Softw 2010;41:427–432.
[16] Wang S, de Sturler E, Paulino GH. Large-scale topology optimization using preconditioned Krylov subspace methods with recycling. Int J Numer Methods Eng 2007;69(12):2441–68.
[17] Kalpakjian S, Schmid S. Manufacturing engineering and technology. New Jersey: Prentice Hall; 2006.
[18] Haftka RT, Gürdal Z, Kamat MP. Elements of structural optimization. Dordrecht: Kluwer Academic; 1992.
[19] Svanberg K. The method of moving asymptotes – a new method for structural optimization. Int J Numer Methods Eng 1987;24:359–73.
[20] Bathe KJ. Finite element procedures. New Jersey: Prentice Hall; 1996.
[21] Bendsøe MP. Optimal shape design as a material distribution problem. Struct Optim 1989;1:193–202.
[22] Zhou M, Rozvany GIN. The COC algorithm, part II: topological, geometry and generalized shape optimization. Comput Methods Appl Mech Eng 1991;89(1):197–224.
[23] Bourdin B. Filters in topology optimization. Int J Numer Methods Eng 2001;50:2143–58.
[24] Zhou M, Shyy Y, Thomas H. Checkerboard and minimum member size control in topology optimization. Struct Multidisc Optim 2001;21(2):152–8.
[25] Almeida SRM, Paulino GH, Silva ECN. A simple and effective inverse projection scheme for void distribution control in topology optimization. Struct Multidisc Optim 2009;39:359–71.
[26] Guest JK. Topology optimization with multiple phase projection. Comput Methods Appl Mech Eng 2009;199(1-4):123–35.